Purely refractive transient energy transfer by stimulated Rayleigh-wing scattering

A. Dogariu, T. Xia,* D. J. Hagan, A. A. Said,† and E. W. Van Stryland

Center for Research and Education in Optics and Lasers, University of Central Florida, Orlando, Florida 32816

N. Bloembergen

Division of Applied Sciences, Harvard University, Pierce Hall, Cambridge, Massachusetts 02138

Received April 11, 1996

Two-beam coupling is demonstrated in CS_2 and other transparent Kerr liquids by use of frequency chirped, picosecond 532-nm-wavelength pulses with several polarization combinations. As the temporal delay between pulses is varied within the coherence time, the first pulse always loses energy while the second pulse gains this energy. The transferred energy at a fixed delay varies linearly with irradiance. The results are consistent with energy transfer from transient refractive gratings that are due to stimulated Rayleigh-wing scattering.
 [S0740-3224(97)00504-3]

1. INTRODUCTION

Energy can be scattered from one beam to another in a two-crossed-beam experiment (pump–probe geometry) if a phase shift occurs between the local optical interference pattern and the grating produced in the material through some irradiance-dependent change in the optical properties of the material. The photorefractive effect is the usual example of such an interaction.[1] This, of course, requires mutual spatial and temporal coherence of the two beams. In pulsed experiments the transient energy transfer that occurs from absorptive gratings leads to what are commonly referred to as coherent artifacts.[2–5] These coherent artifacts occur near zero temporal delay between the pulses (within the temporal coherence time) and transfer energy from the stronger to the weaker beam. If, however, the real part of the refractive index induces the grating, the phase grating can lead to coherent energy transfer only if the nonlinearity has a finite relaxation time so as to allow a phase shift (a finite relaxation time is guaranteed to produce absorption gratings).[6–11] Two-beam coupling in Kerr media such as CS_2 was recently associated with stimulated Rayleigh-wing scattering (SRWS)[10,11]; however, for coupling to occur, the beams must have different frequencies.[12,13] The gain of the Stokes beam depends on the frequency shift from the laser-beam frequency.[14] Nondegenerate two-beam coupling was previously reported by Gruneisen *et al.*[15] For energy transfer to occur in the degenerate case, the beams must develop a frequency difference during the interaction. Such a frequency shift can develop during short pulses owing to self and/or cross-phase modulation.[6–9] A similar beam-coupling effect can occur for cw interactions for nonlinearities with slow response times. This can be obtained from a thermal nonlinear response if one of the beams is phase modulated (for example, by modulating the path length of an interferometer arm).[16]

In the pulsed experiments reported here there is only a refractive grating because the reorientational Kerr effect has a finite relaxation time (e.g., 2 ps for CS_2), and energy is always transferred from the first-arriving pulse to the second-arriving pulse independent of the relative irradiances. The frequency shift is obtained by the small chirp present in mode-locked Nd:YAG laser pulses. Thus the phase grating produced at early times has a phase shift with respect to the optical interference pattern at later times, and energy transfer occurs. This leads to an energy transfer that is linearly proportional to irradiance; thus the signal can be observed at irradiances lower than those needed for nonlinearly induced phase modulation. We first observed the effect in nonlinear absorption measurements, where we identified the solvent to be the cause of this coherent artifact. For example, Fig. 1 shows pump–probe data for a dilute solution of silicon naphthalocyanine (SiNc) in toluene, which is known to exhibit strong excited-state absorption.[17] The two-beam coupling from the solvent is clearly seen superimposed on the reverse saturable absorption signal from SiNc. The dashed curve represents the expected absorption signal. The theory used for the fittings in Fig. 1 (solid curves) is described below.

The measurements reported in this paper are performed on CS_2, but the results are valid for any Kerr liquid that has a nonlinear index of refraction with a relaxation time of the order of the laser pulse width (we obtained this coherent signal in other solvents, such as toluene and nitrobenzene). We demonstrate that the interaction follows the polarization dependence of SRWS.[12–15] The only parameters needed for the theoretical model are the nonlinear index n_2, its relaxation time, and the linear chirp of the laser pulse. The first two are well known for CS_2, and the laser chirp is independently measured by first- and second-order autocorrelations.

0740-3224/97/040796-08$10.00

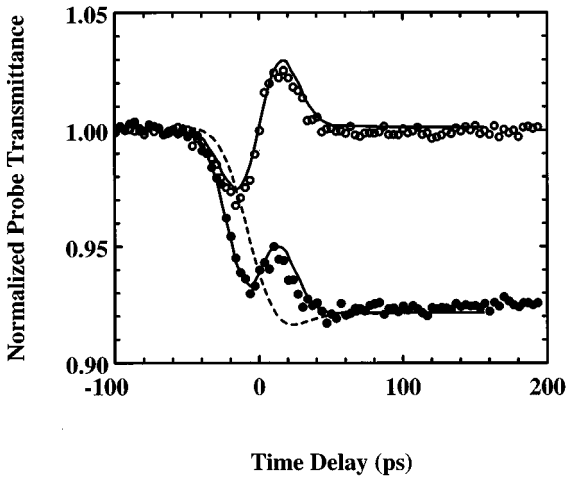

Fig. 1. Normalized probe transmittance as a function of time delay of the probe in toluene (open circles) and in a dilute solution of silicon naphthalocyanine (SiNc) (closed circles) having a linear transmittance of 98.6%. The solid and the dashed curves are theoretical fits (described in the text).

2. THEORY

We assume a laser pulse that has a Gaussian temporal distribution with a time-dependent phase shift and hence a time-dependent frequency shift (i.e., chirp):

$$\mathscr{E}(\mathbf{r}, t) = \mathrm{Re}[A(t)\exp(i\{\mathbf{k}\cdot\mathbf{r} - [\omega + \Delta\omega(t)]t\})], \quad (1)$$

where

$$A(t) = E_0 \exp\left[-\frac{1}{2}\left(\frac{t}{\tau_p}\right)^2\right]. \quad (2)$$

We consider the interaction between two such beams (pump and probe) as derived from the same source. Assume for now that they have the same linear polarization. The probe (subscript p) is temporally delayed by a time τ from the excitation (subscript e). They have the same frequency ω and chirp $\Delta\omega(t)$ but slightly different wave vectors $\mathbf{k}$. Defining the total electric field as

$$E(\mathbf{r}, t, \tau) = A_e \exp(i\{\mathbf{k}_e\cdot\mathbf{r} - [\omega + \Delta\omega(t)]t\}) + \mathbf{A}_p \exp(i\{\mathbf{k}_p\cdot\mathbf{r} - [\omega + \Delta\omega(t-\tau)] \times (t-\tau)\}), \quad (3)$$

the irradiance is given by

$$I = \frac{n_0 c \epsilon_0}{2}|E|^2. \quad (4)$$

With $\mathbf{q} = \mathbf{k}_e - \mathbf{k}_p$ and $\Omega(t, \tau) = \Delta\omega(t) - \Delta\omega(t-\tau)$ the expression for irradiance becomes

$$I = \frac{n_0 c \epsilon_0}{2}[A_e A_e^* + A_p A_p^* + (A_e A_p^* \exp(i\mathbf{q}\cdot\mathbf{r}) \times \exp\{-i[\omega + \Delta\omega(t-\tau)]\tau\}\exp(-i\Omega t) + \text{c.c.})]. \quad (5)$$

Assuming that the frequency shift $\Delta\omega$ is very small compared with the frequency ω, we find

$$I \cong \frac{n_0 c \epsilon_0}{2}\{A_e A_e^* + A_p A_p^* + [A_e A_p^* \exp(i\mathbf{q}\cdot\mathbf{r}) \times \exp(-i\omega\tau)\exp(-i\Omega t) + \text{c.c.}]\}. \quad (6)$$

The grating formed by this interference pattern scatters the beams through a refractive-index variation. We suppose that the refractive nonlinear response obeys a Debye relaxation equation:

$$\tau_{\mathrm{rot}}\frac{dn_{\mathrm{NL}}}{dt} + n_{\mathrm{NL}} = n_2 I, \quad (7)$$

where τ_{rot} is the rotational lifetime, i.e., the time it takes for the nonlinear refractive index to reach its steady state. Solving this equation, the nonlinear refractive index is given by

$$n_{\mathrm{NL}}(t) = \frac{n_2}{\tau_{\mathrm{rot}}}\int_{-\infty}^{t} I(t')\exp[(t'-t)/\tau_{\mathrm{rot}}]dt'. \quad (8)$$

Assuming that the relaxation lifetime is smaller than the pulse width, we can make the approximation that $A(t)$ and $\Omega(t)$ vary more slowly than $\exp[(t'-t)/\tau_{\mathrm{rot}}]$, so the slowly varying amplitude and phase approximation can be used. This approximation holds very well for CS_2 for the 17-ps half-width at $1/e$ maximum in irradiance (HW1/eM) pulse width used, since the rotational lifetime is 2.2 ps.[18] For other materials such as nitrobenzene ($\tau_{\mathrm{rot}} > 40$ ps) or for smaller pulse widths the integrals must be performed numerically. With this approximation the nonlinear refractive index becomes

$$n_{\mathrm{NL}} = \frac{n_0 n_2 c \epsilon_0}{2}\left\{(|A_e|^2 + |A_p|^2) + \frac{A_e A_p^* \exp[i(\mathbf{q}\cdot\mathbf{r} - \Omega t)]\exp(-i\omega\tau)}{1 - i\Omega\tau_{\mathrm{rot}}} + \text{c.c.}\right\}. \quad (9)$$

The total electric field must satisfy the wave equation

$$\nabla^2 E - \frac{1}{c^2}\frac{\partial^2(n^2/E)}{\partial t^2} = 0, \quad (10)$$

where

$$n^2 = (n_0 + n_{\mathrm{NL}})^2 \cong {n_0}^2 + 2n_0 n_{\mathrm{NL}}. \quad (11)$$

Also, because the angle between the beams is small ($\cong 3°$) and because the length of the sample is much smaller than the Rayleigh range, the beams can be considered as copropagating and $\nabla^2 \cong d^2/dz^2$. Putting expression (3) for the total electric field into the wave equation and keeping in mind that $\Omega \ll \omega$, the terms that oscillate as $\exp[i(\mathbf{k}_p\cdot\mathbf{r} - \omega t)]$ (the probe beam) are given by

$$\frac{d^2}{dz^2}\left(A_p \exp\{i[k_p z - \omega(t-\tau)]\}\right)$$

$$= \frac{{n_0}^2}{c^2}\frac{\partial^2}{\partial t^2}\left(A_p \exp\{i[k_p z - \omega(t-\tau)]\}\right) + \frac{{n_0}^2 n_2 \epsilon_0}{c}\frac{\partial^2}{\partial t^2}\left(\left(|A_e|^2 + |A_p|^2 + \frac{|A_e|^2}{1 + i\Omega\tau_{\rm rot}}\right)A_p \exp\{i[k_p z - \omega(t-\tau)]\}\right). \quad (12)$$

We ignore derivatives of the amplitude and the phase by applying the slowly varying amplitude and phase approximation [e.g., $d\Omega/dt \ll 1/(\tau_p \tau_{\rm rot})$] to reduce Eq. (12) to

$$\frac{dA_p}{dz} = \frac{i n_0 n_2 \epsilon_0 \omega}{2}\left(|A_e|^2 + |A_p|^2 + \frac{|A_e|^2}{1 + i\Omega\tau_{\rm rot}}\right)A_p . \quad (13)$$

If we take the derivative of Eq. (4), we obtain for the probe-beam irradiance I_p

$$\frac{dI_p}{dz} = \frac{n_0 c \epsilon_0}{2}\left(\mathbf{A}_p^* \frac{dA_p}{dz} + A_p \frac{dA_p^*}{dz}\right). \quad (14)$$

With Eq. (13) in Eq. (14) and using Eq. (4), we obtain the equation for the probe-beam gain:

$$\frac{dI_p}{dz} = \frac{n_2 \omega}{c} I_e I_p \frac{2\Omega\tau_{\rm rot}}{1 + (\Omega\tau_{\rm rot})^2}. \quad (15)$$

For linearly chirped pulses the input electric field becomes

$$E(\mathbf{r}, t) = E_0 \exp[i(\mathbf{k}\cdot\mathbf{r} - \omega t)]\exp\left[-\frac{1}{2}\left(\frac{t}{\tau_p}\right)^2 (1 + iC)\right], \quad (16)$$

where C is the linear-chirp coefficient.[19] Comparing with Eq. (1) and the definition of Ω, we find the frequency difference, $\Omega = C\tau/{\tau_p}^2$, a constant. With this, Eq. (15) for the gain becomes

$$\frac{dI_p}{dz} = \alpha g I_e I_p ,$$

where

$$g = \frac{n_2 \omega}{c}\frac{2\Omega\tau_{\rm rot}}{1 + (\Omega\tau_{\rm rot})^2}. \quad (17)$$

The weighting coefficient α was introduced for the more general case when the two beams have different polarization, and it is equal to 1 when the beams have the same parallel polarization.[20] The gain g of the SRWS process can be either positive or negative depending on the time delay τ between the pulses. Hence the earlier pulse (with a negative delay) encounters loss, whereas the later pulse (with a positive delay) experiences gain in the interaction. The energy transfer can be understood from Fig. 2. For a negative time delay τ (probe before the pump), because of the linear chirp, the probe beam has a higher frequency than the pump beam does, such that the first beam loses the energy that the second one gains. If the chirp were reversed, the energy transfer would also be reversed.

The signal measured in the delayed pump–probe experiment is given by the normalized total energy of the probe beam after the interaction with the excitation beam:

$$\text{signal}(\tau) = \frac{E_{p,\rm out}}{E_{p,\rm in}} = \frac{2\pi\int_{-\infty}^{\infty} dt \int_0^{\infty} r\,dr I_p}{2\pi\int_{-\infty}^{\infty} dt \int_0^{\infty} r\,dr I_{p0}}, \quad (18)$$

where I_{p0} is the probe irradiance in the absence of the excitation pulse.

For a Gaussian input pulse we obtain from Eqs. (17) and (18) (ignoring pump depletion)

$$\text{signal}(\tau) = \frac{2}{\sqrt{\pi}}\int_{-\infty}^{\infty}\int_0^{\infty} y \exp(-x^2 - y^2) \times \exp\left\{\alpha\Delta\Phi_0 \frac{2\tau/t_m}{1 + (\tau/t_m)^2} \times \exp[-(x - \tau/\tau_p)^2]\exp[-(y r_{pe})^2]\right\} dy\,dx, \quad (19)$$

where $t_m = {\tau_p}^2/(C\tau_{\rm rot})$, $x = t/\tau_p$, $y = \sqrt{2}r/w_{p0}$, and $r_{pe} = w_{p0}/w_{e0}$, the ratio between the probe and excitation beam waists. The SRWS signal depends on the nonlinear phase shift $\Delta\Phi_0 = k n_2 I_{e(r=0,\, t=0)} L$, where L is the sample length (smaller than the Rayleigh range).

In all the figures we used numerical codes in generating the theoretical curves so as to avoid approximations. However, for understanding the shape of the SRWS signal it is useful to make some approximations to obtain a simple form for the signal. For a small signal we can obtain a first-order approximation of the integral form of Eq. (17) that governs the gain. With this approximation the probe irradiance after the interaction becomes

$$I_p = I_{p0}\left[1 + \alpha\Delta\Phi_0 \frac{2\Omega\tau_{\rm rot}}{1 + (\Omega\tau_{\rm rot})^2}\right], \quad (20)$$

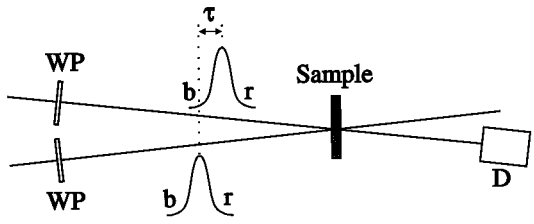

Fig. 2. Excite–probe experimental setup. Detector D measures the probe beam transmittance. Both beams are linearly chirped; b and r represent the blue and red shifts. The earlier pulse interacts with the higher frequency part of its spectrum, whereas the later pulse interacts with the lower-frequency part.

where $I_{p0}(t,\ \tau) = I_{p0}\ \exp\{-[(t\ -\ \tau)/\tau_p]^2\}\exp[-2(r/w_{p0})^2]$ is the input probe irradiance, delayed from the excitation by τ. Integrating Eq. (20) in time and space we obtain the signal

$$\begin{aligned}\text{signal}(\tau) &= 1\ +\ \frac{\alpha\Delta\Phi_0}{(1\ +\ r_{pe}{}^2)\sqrt{2}}\ \frac{2\Omega\tau_{\text{rot}}}{1\ +\ (\Omega\tau_{\text{rot}})^2}\\ &\quad\times\ \exp\left[-\frac{1}{2}\left(\frac{\tau}{\tau_p}\right)^2\right]\\ &= 1\ +\ \frac{\alpha\Delta\Phi_0}{(1\ +\ r_{pe}{}^2)\sqrt{2}}\ \frac{2\tau/t_m}{1\ +\ (\tau/t_m)^2}\\ &\quad\times\ \exp\left[-\frac{1}{2}\left(\frac{\tau}{\tau_p}\right)^2\right].\end{aligned}\tag{21}$$

This expression for the SRWS signal shows that its shape is that of a derivative of a Lorentzian $[2x/(1\ +\ x^2)]$ weighted by a Gaussian $\{\exp[-(x/a)^2]\}$. The small-signal approximation works very well for our experimental data for CS_2. It is easy also to obtain Eq. (21) directly from Eq. (19) within the stated approximation, i.e., by expanding the exponential function of time delay. It is interesting to observe that the substitution we have made, $t_m = \tau_p{}^2/(C\tau_{\text{rot}})$, represents the time when the derivative of the Lorentzian is maximum, and it would represent also the time when the signal peaks for quasi-cw beams (pulse width much longer than t_m). On the other hand, for pulses much shorter than t_m, the signal peaks at a time equal to the pulse width τ_p. This is easy to show by taking the derivative of Eq. (21) to obtain the time delays for which the signal has a maximum and a minimum. Hence, for $\tau_p/t_m \gg 1$ and $\tau_p/t_m \ll 1$, we obtain

$$\tau_{\text{max,min}} \cong \pm\frac{\tau_p t_m}{\sqrt{\tau_p{}^2\ +\ t_m{}^2}},\tag{22}$$

which gives t_m for long pulses and τ_p for short pulses (relative to t_m).

3. EXPERIMENT

The source for the delayed pump–probe experiment is the second harmonic of a Nd:YAG Q-switched mode-locked laser with a pulse width of 17 ps (HW1/eM) at 532 nm. The laser repetition rate is 10 Hz. The experimental setup is given in Fig. 2. The energy of the beams is adjusted by rotating a half-wave plate situated before a polarizer. The second harmonic (532 nm) is then split into the pump and the probe beams. The pump beam is then focused by a 100-cm focal-length lens onto the sample so that the waist of the beam in the sample is 100 μm (HW1/e^{2}M). The probe beam is delayed by a system of two corner cubes and a mirror, with one of the corner cubes on a stage. The probe beam is focused to 20 μm (HW1/e^{2}M) by a 20-cm focal-length lens such that r_{pe} = 1/4. Both beams are focused onto the 1-mm-thick sample. The angle between the beams is 3°. The excitation beam has 10 times the probe irradiance (160 times the energy); thus the probe beam does not induce any significant nonlinearity. Using appropriate wave plates (WP's), we can perform the experiments with several polarization combinations for the pump and the probe beams.

The signal showing the coherent two-beam coupling can be seen, for example, in Fig. 3. To study this signal, we performed experiments on CS_2. To check that the energy transfer was due to SRWS, we had to prove that the magnitude of our signal followed the polarization dependence of any SRWS signal. The scattering process in an isotropic medium follows the ratios 4:3:6:1 for scattering with parallel (or perpendicular) linear polarization inputs and with opposite (or same) circular polarization inputs, respectively (see Table 1).[12,13,20,21] We performed pump–probe measurements using these polarization combinations for the excitation and the probe beams. The theoretical curves (solid curves in figures) were generated with the polarization coefficient α introduced in Eq. (17). A comparison between the measured and the predicted polarization dependences is illustrated Table 1.

We used the polarization coefficient for the linear but perpendicularly polarized measurement (i.e., α = 0.75) as the reference in scaling the other coefficients, since this measurement had the best signal-to-noise ratio.

A strong argument that the frequency difference needed ($\Omega \neq 0$) for the SRWS is due to linear chirp and not due to other nonlinear processes is shown by the data of Fig. 4. Figure 4 is a plot of the magnitude of the SRWS signal, ΔT_{pv}, (the difference between the peak and the valley of the signal) as a function of the excitation irradiance. We can see that the signal is linear in irradiance up to 4 GW/cm^2 (which corresponds to a nonlinear phase shift $\Delta\Phi_0$ = 1.7). The theoretical line from Fig. 4 is generated by the following formula, obtained from Eqs. (21) and (22) with $\tau_{\text{max,min}} \cong \tau_p$:

$$\Delta T_{pv} = 2\sqrt{2}\ \exp(-1/2)\ \frac{\alpha\Delta\Phi_0 C\tau_{\text{rot}}}{\tau_p}.\tag{23}$$

Because the signal measured has a linear and not a higher-order dependence on the excitation irradiance and because in Eqs. (19)–(21) the nonlinear phase shift $\Delta\Phi_0$ has a linear dependence on irradiance, we know that the frequency difference between the beams Ω has to be independent of irradiance. For any nonlinearly obtained chirp, Ω would be irradiance dependent, and the signal would have a higher-order irradiance dependence. As expected, at higher irradiances (e.g., $I_{e0} > 4$ GW/cm^2) the nonlinear processes of self- and cross-phase modulation further chirp the pulses, altering this linear dependence.

With the known nonlinear refractive index $n_2 = 3.1 \times 10^{-14}$ cm^2/W (Ref. 22) and rotational lifetime τ_{rot} = 2.2 ps,[20] the only fitting parameter needed is the linear-chirp coefficient, C. For all the curves generated in Fig. 3 we used C = 0.75. To independently measure the linear chirp of the pulses, we performed first- and second-order autocorrelations on the input beam. The second-order autocorrelation was a usual Michelson interferometer that, by use of second-harmonic generation, gave us the pulse width τ_p = 17 ps (HW1/eM). Using the same setup, but without the second-harmonic crystal, one can determine the coherence time of the pulse by measuring the first-order autocorrelation (correlation of

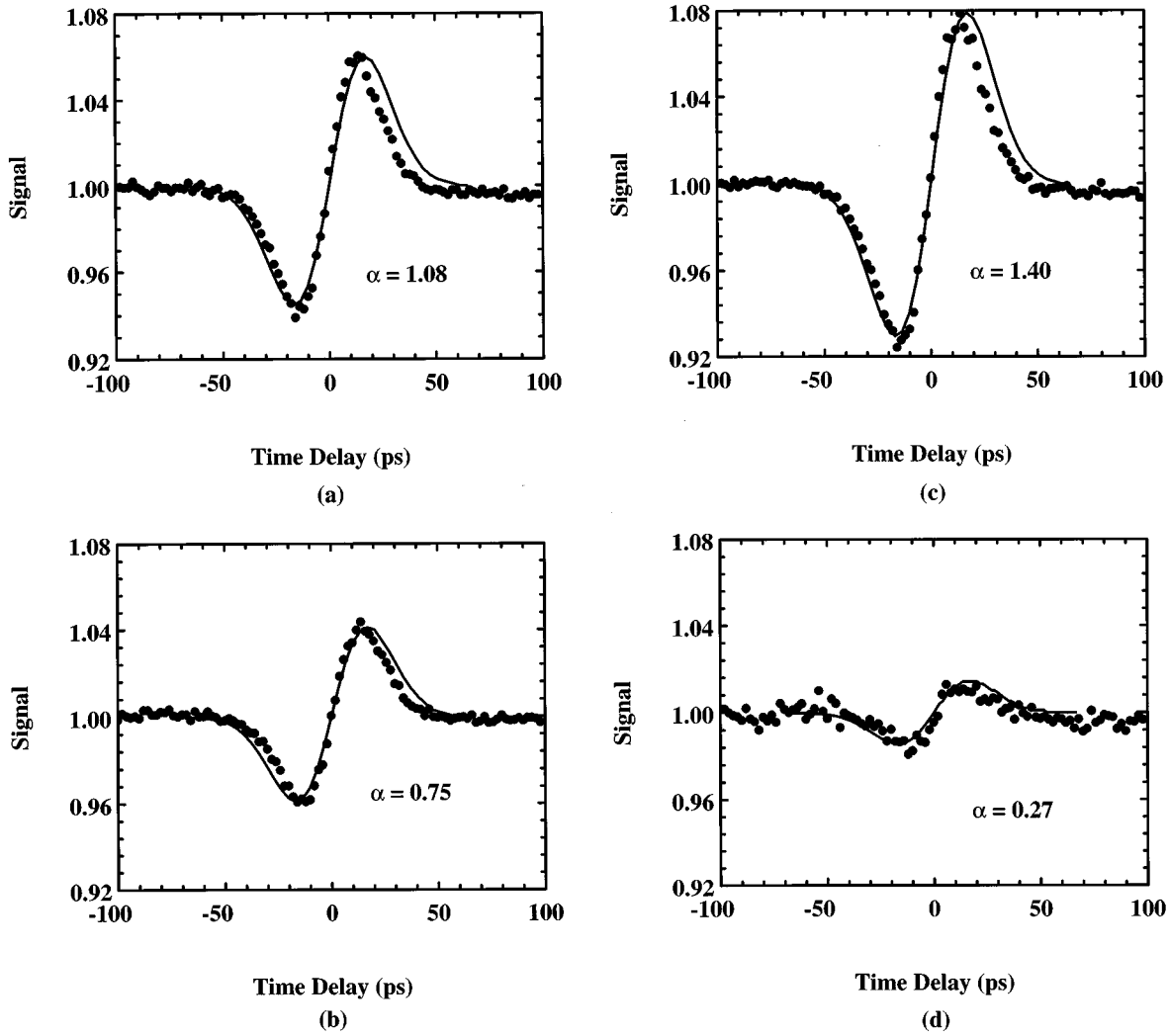

Fig. 3. SRWS signal dependence on polarization: (a) parallel-linear, (b) perpendicular-linear, (c) opposite-circular, and (d) same-circular polarization. Experimental conditions: $I_{10} = 1.9$ GW/cm^2 and $\tau_p = 17$ ps. The circles are experimental data; solid curves represent theoretical fits assuming a linear chirp, $C = 0.75$.

Table 1. Relative Signal for Different Polarization Combinations

Polarization	α (Experiment)	α (Theory)
Parallel linear	1.08	1.00
Perpendicular linear	0.75	0.75
Opposite circular	1.40	1.50
Same circular	0.27	0.25

the electric field with itself). This can be done by measuring the fringe visibility. In Fig. 5 we can see how the interference pattern changes with time delay at 1.06 μm. By plotting the contrast of the pattern (i.e., minima and maxima) as a function of time delay, we obtain the envelope of the first-order autocorrelation function. For a Gaussian pulse, the width of this is a factor of 2 larger than the coherence time. This gives a coherence time of 19.4 ps (HW1/eM) at 1.06 μm, which infers a coherence time of 13.7 ps (HW1/eM) at 532 nm (Fig. 6). This is less

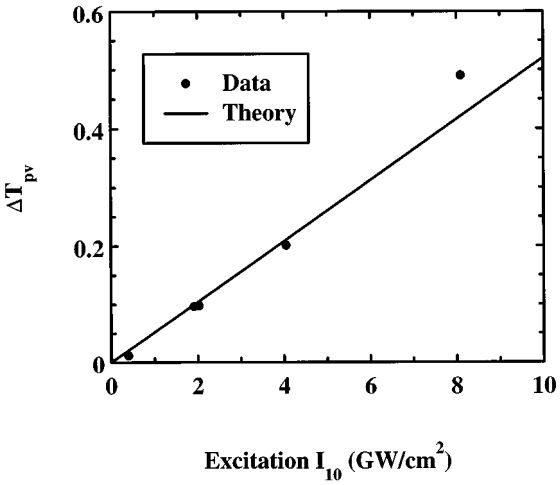

Fig. 4. Magnitude of the SRWS signal (difference between peak and valley) as a function of excitation irradiance (circles). The theoretical curve is generated by Eq. (23) with the same value for linear chirp used in fitting the data from Fig. 3.

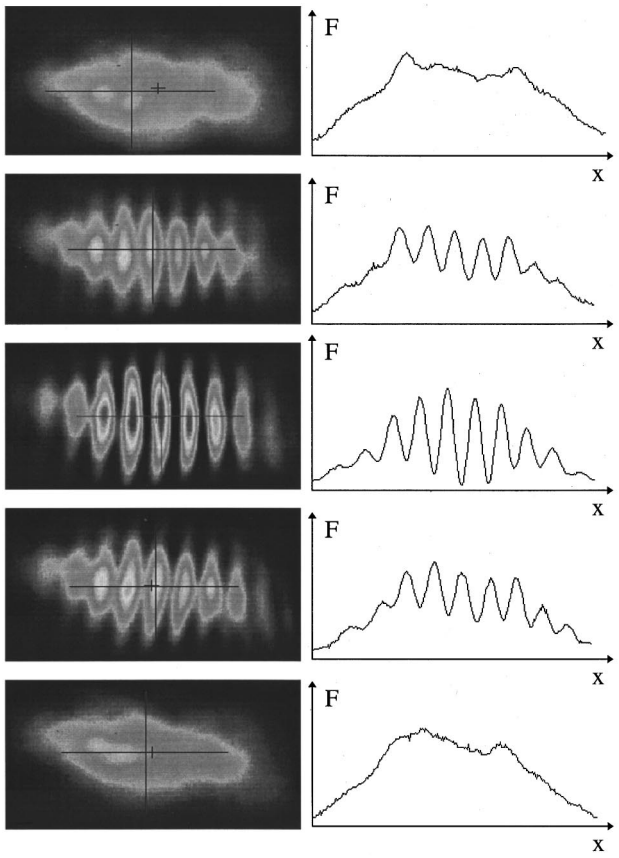

Fig. 5. Interference pattern given by first-order autocorrelation for (from top to bottom) −120-, −46.6-, 0-, 46.6-, and 120-ps time delay at 1.06 μm.

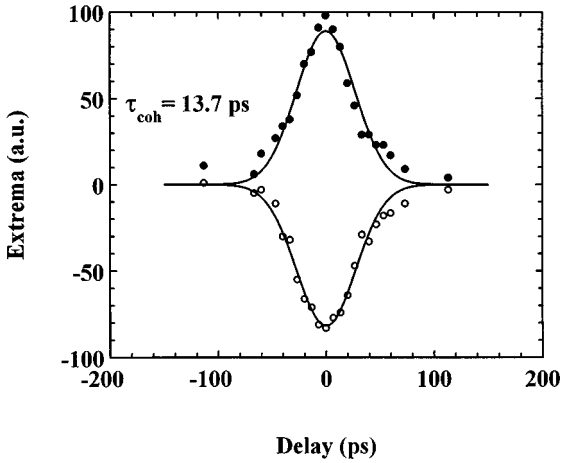

Fig. 6. Maxima (filled circles) and minima (open circles) of the interference pattern from Fig. 5 as a function of time delay. The solid curve is a Gaussian fit giving the coherence time of the pulses, τ_{coh} = 13.7 ps (HW1/eM) at 532 nm.

than the 17-ps (HW1/eM) pulse width, indicating chirp. Assuming a linear chirp,[19]

$$\tau_p = \tau_c\sqrt{1 + C^2}. \tag{24}$$

This method gives us the chirp coefficient $C = 0.73$, very close to the one used for generating the theoretical fits of the SRWS signal.

To further test the signal dependence on the linear chirp, we changed the laser pulse width from 17 ps to 25 ps (HW1/eM) by replacing the étalon that is the output coupler of the laser cavity. By doing so, we decreased the chirp of the pulses. Indeed, the chirp coefficient used to

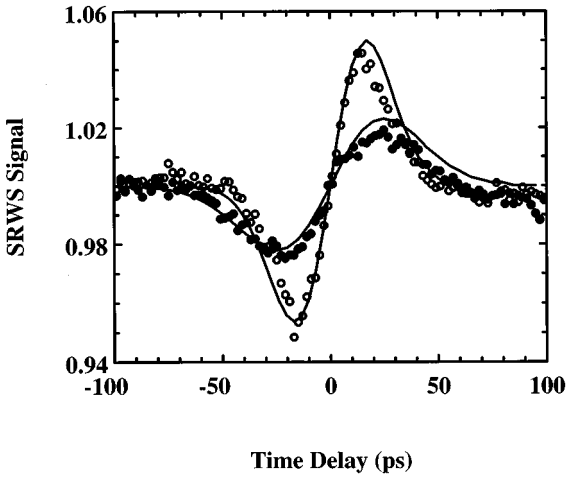

Fig. 7. SRWS signal for different laser pulse widths: 17 ps (open circles) and 25 ps (filled circles). The values for the linear-chirp coefficient used in fitting the data are $C = 0.85$ for the 17-ps pulse and $C = 0.6$ for the 25-ps pulse.

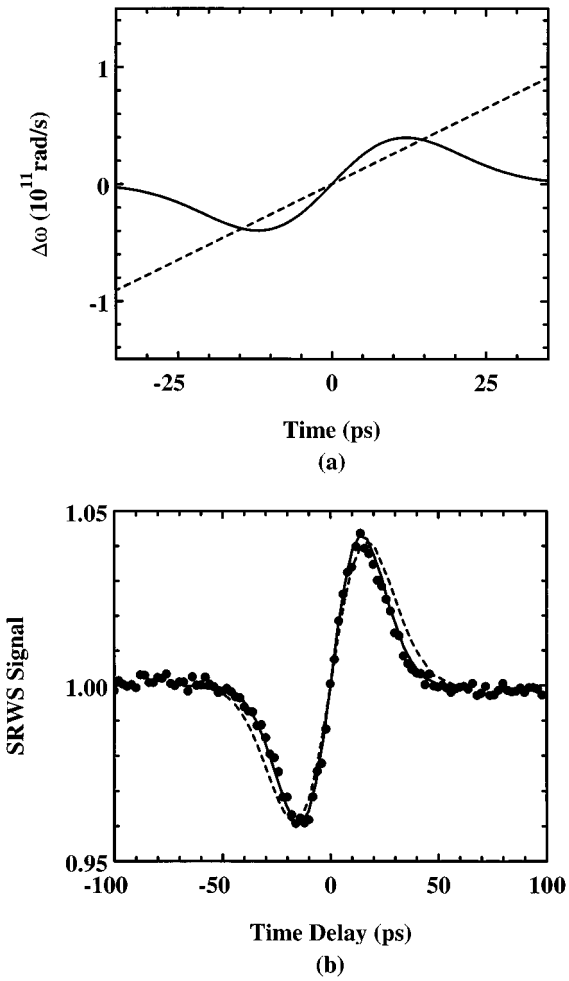

Fig. 8. (a) Linear chirp weighted by the Gaussian pulse (solid curve) and the linear chirp by itself (dashed curve) (b) are used for fitting the data (filled circles).

fit the data from Fig. 7 changes from 0.85 to 0.6 for the longer pulse. Note that this particular measurement was performed six months after the rest of the measurements. Hence the use of a different mode-locking dye and lasing threshold in the laser cavity could explain the different chirp coefficient needed to fit the data (0.85 instead of 0.75 as before). The signals are obtained for the same input irradiance, $I_{e0} = 1.9$ GW/cm^2. It can be noted that the signal peaks at approximately the predicted values, i.e., the pulse widths: ± 17 ps and ± 25 ps.

Although the theoretical curves simulate the data very well, there is a small discrepancy, which is that the signal does not peak exactly where the theory predicts. As discussed before, in the case in which the pulse width τ_p (in our case, 17 ps) is much smaller than t_m (in our case, $\cong$175 ps), the peaks should be at $\pm\tau_p$. Our data always peak at approximately ± 13 ps. This fact can be easily explained if we consider a more realistic case for the laser pulse chirp. If the chirp is obtained in the laser cavity by nonlinear processes, it will follow the temporal shape of the pulse. So if we alter the chirp by considering the linear chirp weighted by a temporal Gaussian, we can see that the curve shrinks in time so that we get a better fit to the data (Fig. 8). The equations used before are no longer valid, and numerical routines have to be used to generate the curves. However, all the physical considerations about the linearity in irradiance and polarization dependence remain valid.

4. CONCLUSION

It is often assumed that purely refractive gratings will not lead to energy transfer in pulsed degenerate pump–probe experiments because of the lack of a phase-shifting mechanism such as exists in photorefractive media by means of the electro-optic effect. We have demonstrated coherent energy transfer using refractive gratings for identical pulses in the degenerate case but with weakly chirped pulses and at irradiances low enough that self-phase modulation and cross-phase modulation can be neglected with 532-nm, picosecond pulses. The two beam coupling takes place in Kerr-type media with a slow nonlinear refractive index. The material remembers the grating written during the first part of the pump–probe interaction, which then scatters different frequencies at later times into the pump or probe directions, depending on which pulse is first. The phase shifting mechanism here is simply due to the different frequencies present at different times in the pulses, i.e., chirp. The memory effect is due to SRWS, and the polarization dependence of the interaction is in agreement with theoretical predictions. In the case of CS_2 for a usual pump–probe experiment a simple formula can be used successfully to fit this coherent effect, which depends on the product of the nonlinear refractive index n_2, the rotation relaxation time τ_{rot}, and the linear chirp coefficient C. Knowledge of any two of these parameters allows calculation of the third. The linear chirp is independently measured with first- and second-order autocorrelations, and the linear chirp found in this way is the same within experimental error as that calculated from the known n_2 and τ_r. Knowing the linear chirp of the laser pulses, the SRWS signal obtained with a particular material gives information about the response time of the nonlinearity. For example, using appropriate pulse widths, one can distinguish between the reorientational (slow) and the bound electronic (fast) nonlinear refractive index.

As with coherent artifacts from absorptive gratings, these refractive coherent artifacts must be subtracted from data to extract the dynamics of other nonlinearities. As seen in Fig. 1, the solid curve fittings for the corrupted data contain the SRWS signal, while the dashed curve shows the dynamics of the production of the excited-state absorbers alone.

ACKNOWLEDGMENT

We gratefully acknowledge the support of Naval Air Warfare Center Joint Service Agile Program contract N66269-C-93-0256 and National Science Foundation grant ECS 9510046.

*Present address, Department of Electrical Engineering and Computer Science, University of Michigan, Ann Arbor, Michigan 48109.

†Present address, AccuPhotonics, Inc., 2901 Hubbard Road, Ann Arbor, Michigan 48105.

REFERENCES

1. D. Staebler and J. Amodei, "Coupled-wave analysis of holographic storage in $LiNbO_3$," J. Appl. Phys. **43**, 1042 (1972).
2. E. P. Ippen and C. V. Shank, in *Ultrashort Light Pulses*, S. L. Shapiro, ed. Vol. 18 of Topics in Applied Physics (Springer-Verlag, Berlin, 1977), p. 83.
3. A. von Jena and H. E. Lessing, "Coherent coupling effects in picosecond absorption experiments," Appl. Phys. **19**, 131 (1979).
4. Z. Vardeny and J. Tauc, "Picosecond coherence coupling in the pump and probe technique," Opt. Commun. **39**, 396 (1981).
5. B. S. Wherrett, A. L. Smirl, and T. G. Boggess, "Theory of degenerate four-wave mixing in picosecond excitation-probe experiments," IEEE J. Quantum Electron. **19**, 680 (1983), and references therein.
6. S. L. Palfrey and T. F. Heinz, "Coherent interactions in pump-probe absorption measurements: the effect of phase gratings," J. Opt. Soc. Am. B **2**, 674 (1985).
7. D. Rogovin, T. P. Shen, J. Scholl, T. Dutton, and P. Rentzepis, "Polarization-resolved coherent transient beam combination in optical Kerr media," Opt. Lett. **15**, 1132 (1990).
8. T. E. Dutton, R. M. Rentzepis, T. P. Shen, J. Scholl, and D. Rogovin, "Picosecond degenerate two-wave mixing," J. Opt. Soc. Am. B **9**, 1843 (1992).
9. P. S. Spencer and K. A. Shore, "Pump–probe propagation in a passive Kerr nonlinear optical medium," J. Opt. Soc. Am. B **12**, 67 (1995).
10. K. D. Dorkenoo, D. Wang, N. P. Xuan, J. P. Lecoq, R. Chevalier, and G. Rivoire, "Stimulated Rayleigh-wing scattering with two-beam coupling in CS_2," J. Opt. Soc. Am. B **12**, 37 (1995).
11. G. Rivoire and D. Wang, "Dynamics of CS_2 in the large spectral bandwidth stimulated Rayleigh-wing scattering," J. Chem. Phys. **99**, 9460 (1993).
12. R. W. Boyd, *Nonlinear Optics* (Academic, New York, 1992), p. 389.
13. L. D. Landau, E. M. Lifshitz, and L. P. Pitaevskii, *Electrodynamics of Continuous Media* (Pergamon, Oxford, 1960), p. 377.
14. N. Bloembergen and P. Lallemand, "Complex intensity-dependent index of refraction, frequency broadening of

stimulated Raman lines, and stimulated Rayleigh scattering," Phys. Rev. Lett. **16**, 81 (1966).
15. M. T. Gruneisen, K. R. MacDonald, A. L. Gaeta, R. W. Boyd, and D. J. Harter, "Laser beam combining in potassium vapor," IEEE J. Quantum Electron. **27**, 128 (1991).
16. S. Miller, "Ultrasensitive technique for measuring two-photon absorption," Ph.D. dissertation (University of North Texas, Denton, Texas, 1991).
17. T. H. Wei, D. J. Hagan, E. W. Van Stryland, J. W. Perry, and D. R. Coulter, "Direct measurements of nonlinear absorption and refraction in solutions of phthalocyanines," Appl. Phys. B **54**, 46 (1992).
18. E. P. Ippen and C. V. Shank, "Picosecond response of a high-repetition rate CS_2 optical Kerr gate," Appl. Phys. Lett. **24**, 92 (1975).
19. G. Agrawal, *Nonlinear Fiber Optics* (Academic, New York, 1989), p. 58.
20. R. Y. Chiao and J. Godine, "Polarization dependence of stimulated Rayleigh-wing scattering and the optical-frequency Kerr effect," Phys. Rev. **185**, 430 (1969).
21. R. W. Minck, E. E. Hagenlocker, and W. G. Rado, "Stimulated pure rotational Raman scattering in deuterium," Phys. Rev. Lett. **17**, 229 (1966).
22. W. E. Williams, M. J. Soileau, and E. W. Van Stryland, "Optical switching and n_2 measurements in CS_2," Opt. Commun. **50**, 256 (1984).